Understanding the importance of the energetics of Mn, Ni, Cu, Si and vacancy triplet clusters in *bcc* Fe

T. M. Whiting[1], P. A. Burr[2], D. J. M. King[1] and M. R. Wenman[1, a)]

[1] Department of Materials and Centre for Nuclear Engineering, Imperial College London, London, UK

[2] School of Mechanical and Manufacturing Engineering, University of New South Wales, NSW, 2052, Australia

[a)] Author to whom correspondence should be addressed: m.wenman@imperial.ac.uk

Abstract

Numerous experimental studies have found the presence of (Cu)-Ni-Mn-Si clusters in neutron irradiated reactor pressure vessel steels, prompting concerns that these clusters could lead to larger than expected increases in hardening, especially at high fluences late in life. The mechanics governing clustering for the Fe-Mn-Ni-Si system are not well-known; state-of-the-art methods use kinetic Monte Carlo (KMC) parameterised by density functional theory (DFT) and thermodynamic data to model the time evolution of clusters. However, DFT based KMC studies have so far been limited to only pairwise interactions due to lack of DFT data. Here we explicitly calculate the binding energy of triplet clusters of Mn, Ni, Cu, Si and vacancies in *bcc* Fe using DFT to show that the presence of vacancies, Si, or Cu stabilises cluster formation, as clusters containing exclusively Mn and/or Ni are not energetically stable in the absence of interstitials. We further identify which clusters may be reasonably approximated as a sum of pairwise interactions, and which instead require an explicit treatment of the three-body interaction, showing that the three-body term can account for as much as 0.3 eV, especially for clusters containing vacancies.

Keywords: Steel; neutron irradiation; solute; vacancy; clusters

1. Introduction

The key component that dictates the operational lifetime of a pressurised water reactor (PWR), is the reactor pressure vessel (RPV), which is constructed of low-alloy ferritic steel. During steady state operation, the RPV is subject to elevated temperatures (~600 K) and a high energy (>1 MeV) neutron flux that leads to the creation of nano-scale features [1,2]. These features impede dislocation motion, resulting in a hardening of the RPV, and ultimately to an increase in the ductile-to-brittle transition temperature. If this increase is too large, the safety case under accident conditions cannot be justified.

The most common features observed as a result of fast neutron radiation damage in RPV steels are voids, dislocation loops, and solute clusters composed primarily of Si, Ni, Mn and Cu [3–6]. The latter is the focus of a global research effort to gain a mechanistic understanding of solute clustering in RPV steels [7–16]. The aim of this global effort is two-fold, to improve the design of new steel compositions, especially their resistance to radiation-induced solute clustering, and improving current dose damage relationship models at high fluences beyond 40 years operation of a PWR.

Historically, Cu dominated the cluster compositions, especially in the welds of early RPVs leading to their designation as Cu-rich precipitates (CRPs) [2,17–19]. However, in more modern reactors, RPV steels have largely reduced Cu contents (< 0.1 at. %); but clusters of Mn-Ni-Si have been predicted by Monte Carlo simulations based on both thermodynamic models [20–22] and density functional theory (DFT) results [23–26]. These clusters have been observed experimentally at fluences greater than 10^{23} n m^{-2} [3,27–33], and in non-irradiated thermally-aged steel as well [34,35], causing concern for late-life performance of currently operating RPVs. Atom probe tomography studies of these Mn-Ni-Si solute clusters have often found Cu cores surrounded by Ni, Mn, Si enriched shells [5,30,36–38]. However, recent experiments have also found that clusters can develop in the absence of Cu

[3,31,39,40] and solute-vacancy [41,42] and solute-interstitial [43,44] complexes develop in addition to pure solute clusters in both RPV steel and model alloys.

Difficulties exist in trying to elucidate the structures and exact chemical compositions due to the small size of the solute clusters (1-3 nm) and limitations in the analysis techniques, and so there is still debate as to their formation mechanism, chemical compositions (including Fe content) and structure. Therefore investigations into matrix damage and solute clusters using multi-scale modelling techniques are ongoing [14,45–47]. DFT, molecular dynamics (MD) and kinetic Monte Carlo (KMC) are well suited to investigating the thermodynamics, kinetics and structure of such features. Currently, however, there has been limited work on clusters containing more than two solute atoms in the low-alloy ferritic Fe-Cu-Mn-Ni-Si system. Mixed Ni-Mn triplets were studied by Bonny et al., which modelled four distinct triplets (Mn_3, Mn_2Ni, $MnNi_2$, Ni_3) [48] and further studies by Bakaev et al. [49] and Bonny et al. [50] have looked at divacancy containing triplets, and Ni-Cr-vacancy triplets/quadruplets respectively. These results have been further built upon in [51] with studies of more triplet clusters and investigations of cluster expansion. However, these studies have only looked at one configuration of triplets (the triangle or 1-1-2 configuration, as described in this work and with the exception of [50,51], have not varied the ordering within the configuration or quantified the impact of including triplet clusters in KMC codes as opposed to purely pairwise interactions. Further, in the development of quaternary Fe-Mn-Ni-Cu embedded atom potentials, the binding energy of some Mn-Ni pairs and triplets were calculated by DFT to be repulsive [48] and did not adequately reflect the experimentally observed cluster growth. Therefore, these binary solute interactions were empirically modified to be slightly attractive to allow for cluster growth to occur. Additionally, a recent study by Domain and Becquart [14] has found that DFT and MD calculations, using the potentials developed in Ref. [48], are in poor agreement when simulating solutes close to <111> interstitial loops.

Several different KMC models have also been developed to study the evolution due to neutron irradiation of RPV steels, including many atomic species (Cu, Mn, Ni, Si, P, Cr) [23,24,26,52]. These are commonly parameterized by empirical thermodynamic data [20–22,53] or DFT data [24,25,54,55], although other models based on rate-theory [39] and a combination of tight-binding and experimental data [56] have been developed in the past. Disagreement exists between models, with thermodynamic-based KMC suggesting that the clusters are stable and radiation enhanced, whereas DFT-based KMC favours the hypothesis that clusters are radiation induced [25].

There has been particular interest in the role of interstitial driven migration, with much KMC successfully modelling the interactions of dumbbells with solutes; including development of the LAKIMOCA code that emphasises the role of SIAs in solute migration [23–26,54] due to the high binding energy that Mn has been found to exhibit for self-interstitial defects [57,58].

The role of non-pairwise interactions has been thus far absent from the literature and therefore the KMC models. In this study, which was performed concurrent to one by Bonny *et al.* [51], the energetic influence of triplet clusters is investigated using DFT. In the study by Bonny *et al.* DFT was used to expand on the previous work on solute pairs that are currently used to parametrise higher order codes that incorporate time evolution (KMC and MD) [23–26,47], and to determine the effect of three-body interactions on solute triplets, when compared to energies calculated by only taking into account pairwise interactions. Here, we analyse the triplet clusters in detail to show, which configurations are the lowest energy and furthermore to study the errors that are incurred in trying to represent these 3-body interactions as 2-body interactions not reported in [48].

2. Method

DFT calculations were performed using the Vienna *ab initio* simulation package (VASP) [59–62]; a plane-wave code that implements the projector augmented wave method (PAW) [60,63], which has

been used with the Perdew-Burke-Ernzerhof (PBE) exchange-correlation functional, based on the generalised gradient approximation [64]. For the elements Fe, Cu, Ni, Mn and Si, pseudopotentials included within the VASP 5.4 distribution were used with 14, 17, 16, 13 and 4 valence electrons, respectively. Brillouin zone sampling was performed using the Monkhorst-Pack scheme, where a *k*-point mesh of 4×4×4, a cut-off energy of 500 eV and Methfessel-Paxton [65] smearing (with a width of 0.1 eV) proved sufficiently converged to 10^{-3} eV for the pure elements. The tetrahedron smearing method with Blöchl corrections [63] was used on fixed dimension/volume calculations to generate the density of states (DOS). Supercells were constructed and fully relaxed using constant pressure calculations; using 128 atom (4×4×4 bcc Fe unit cells) a lattice parameter of 2.831 Å was calculated to be ground-state. Supercell convergence tests using 256, 128, 54 atoms were performed, from which it was found that 128 atom cells are adequate for modelling substitutional triplet clusters. Constant volume relaxations of the supercells with the defect clusters were performed to obtain binding energies. All variations of Mn-Mn-X, Mn-Ni-X, Ni-Ni-X where X is Cu, Mn, Ni, Si or a vacancy were considered, as well as all clusters containing one or two vacancies (vacancy-X-X and vacancy-vacancy-X). The electronic energy and ionic relaxation convergence criteria were set to 10^{-6} and 10^{-4} eV, respectively, for all calculations.

Binding energies for solute-vacancy triplets were calculated using:

$$E_b(X_1, X_2, X_3) = E(\textstyle\sum_{i=3} X_i) - \sum_{i=3} E(X_i) + 2E(\mathrm{Fe}) \quad (1)$$

where $E(\mathrm{Fe})$ is the energy of a pure Fe supercell, $E(X_i)$ is the energy of the supercell containing a single solute and $E(\sum_i X_i)$ is the energy of the supercell containing all solutes.

The binding energy of a triplet can be described as the sum of the pairwise interaction plus a three-body term

$$E_b(X_1, X_2, X_3) = E_b(X_1, X_2; n_{1-2}) + E_b(X_2, X_3; n_{2-3}) + E_b(X_3, X_1; n_{3-1}) + E^{\text{3-body}}(X_1, X_2, X_3) \quad (2)$$

where $E_b(X_i, X_j; n_{i-j})$ is the pair binding energy of solutes X_i and X_j at $n_{i\text{-}j}$ nearest neighbour separation. Thus, Eq. (2) was used to calculate the magnitude of the three-body term, $E^{\text{3-body}}$. The binding energy of the triplet, when only taking pairwise interactions into account, was calculated using Eq. (3).

$$E_b^{\text{2-body}}(X_1, X_2, X_3) = E_b(X_1, X_2; n_{1-2}) + E_b(X_2, X_3; n_{2-3}) + E_b(X_3, X_1; n_{3-1}) \quad (3)$$

The pairwise triplet binding energy from Eq. (3) was then compared to the exact binding energy from the explicit DFT calculation of the triplet.

$$E^{\text{3-body}}(X_1, X_2, X_3) = E_b(X_1, X_2, X_3) - E_b^{\text{2-body}}(X_1, X_2, X_3) \quad (4)$$

Under these definitions, negative energy represents attractive binding.

3. Results and discussion

3.1 First to fifth nearest neighbour pairs

The binding energies between each solute species in the *bcc* Fe lattice provides insight into local stabilities and potential migration behaviour. Fig. 1 shows the interactions of solute pairs (of same species) and solute-vacancy pairs from first nearest neighbour (1nn) to fifth nearest neighbour (5nn); there is good agreement with previous works, with the exception of Mn for which there is a large spread of reported results. Discrepancies associated with Mn are due to the shallow energy landscape between ferromagnetic and antiferromagnetic moments (AFM) leading to differences in isolated reference states and variations in the magnetic moment in the pairs. These findings were reported in a previous publication [66]. According to the findings, all Mn atoms were given the initial magnetic

moment of (-2 μ_B) corresponding to the AFM coupling to Fe. The decrease in binding energy between a vacancy and Cu, Mn and Ni at 5nn (compared to 4nn) is attributed to the "Friedel like" relaxation around a vacancy in Fe. The 5nn sites are in a compressive region (compared to tensile of the 4nn configuration) [57].

Fig. 2 compares the binding energies between Cu, Mn, Ni and Si defects from 1nn to 5nn, together with past literature results. Inconsistencies in our results with Vincent *et al.* [67] are attributed to the use of Vanderbilt-type ultra-soft pseudopotentials used by Vincent *et al.* that do not describe well the strongly varying core part of the *d*-like orbitals compared to the PAW electronic methods used in this work. It is evident from Fig. 2 that there is non-negligible binding between Si and other solute elements (top row), which may be important for cluster dynamics. Specifically, Si exhibits both a strong binding at 1nn with Mn, Cu and Ni (~ -0.15 eV), and a repulsion at 2nn with Ni and Mn (~0.10 eV). In agreement with Olsson *et al.*[57], interactions beyond 2nn are very small, due to the increased separation and suggesting that efforts should be concentrated on modelling the energetics of 1nn and 2nn solute pairs in particular. Olsson *et al*. note that large changes in solute-vacancy binding energies (~ 0.2 eV) between 1nn and 2nn, as are observed here for both solute-vacancy and Si-solute interactions, can be explained by large differences in charge distribution surrounding vacancies in *bcc* Fe [57]. The exact configuration and co-ordination of small clusters is important when modelling cluster growth in KMC codes as there are 8, 6, 12, 24 and 8 possible sites for 1nn, 2nn, 3nn, 4nn and 5nn positions respectively in the *bcc* lattice.

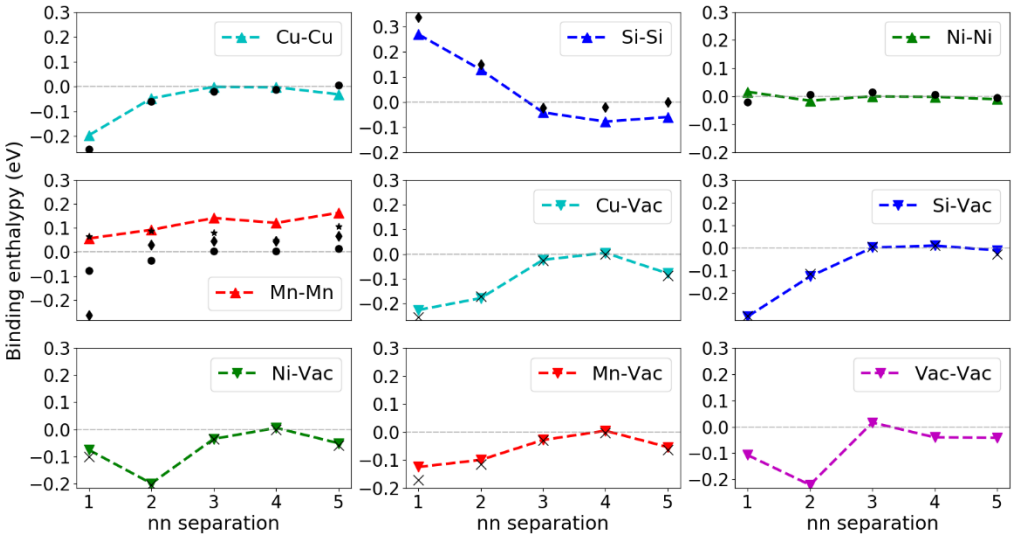

Fig. 1 *Binding enthalpy of same solute and solute-vacancy pairs obtained by supercell relaxations, compared with previous works by Messina et al.* [13] *(crosses), Bakaev et al.* [68] *(diamonds), King et al.(stars)* [66] *and Olsson et al. (circles)* [57].

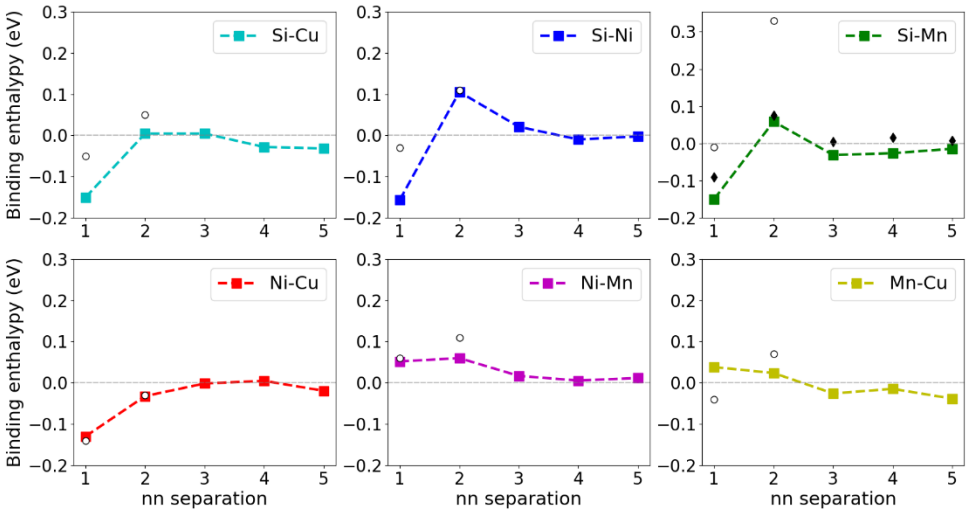

Fig. 2 *Binding enthalpy of mixed solute pairs obtained by supercell relaxations, compared with previous works by Vincent et al.* [67] *(white circles) and Bakaev et al.* [68] *(black diamonds).*

3.2 Mn-Ni Triplets

In this section work is presented on triplet clusters in which at least two of the defects are Mn or Ni, and the other is either Si, Cu, Mn, Ni or a vacancy. Due to the pronounced 1nn interactions in the binary cases, triplet calculations have focused on geometries where one of the atomic species in the triplet cluster is 1nn to both of the other solutes. These configurations are termed 1-1-2, 1-1-3 and 1-1-5, where for the triplet composed of species A, B and C in the a-b-c configuration: a is the nearest neighbour number of B relative to A, b is the nearest neighbour number of C relative to B and c is the nearest neighbour number of A relative to C as shown in Fig. 3. For each triplet configuration and composition, we consider all possible permutations of species on each site. Therefore, triplet clusters with three different species will have three discrete energies for each configuration (1-1-2, 1-1-3 and 1-1-5) for a total of nine discrete energies for that cluster chemistry; but due to symmetry, triplets with two different species (eg. Mn-Mn-Ni) will have two possible energies per configuration and triplets with one species (eg. Mn-Mn-Mn) have only one energy per configuration. Higher order interactions such as quadruplet and quintuplet clusters have been omitted due to the expense of DFT calculations and the vast multiplicity involved with modelling these clusters. Additionally, as there already exists substantial literature on interactions of solutes with interstitial dumbbells in various positions [23–26,54], in this work we have concentrated instead on the role of Cu, Si and vacancies in stabilising triplet clusters of different geometries in substitutional positions.

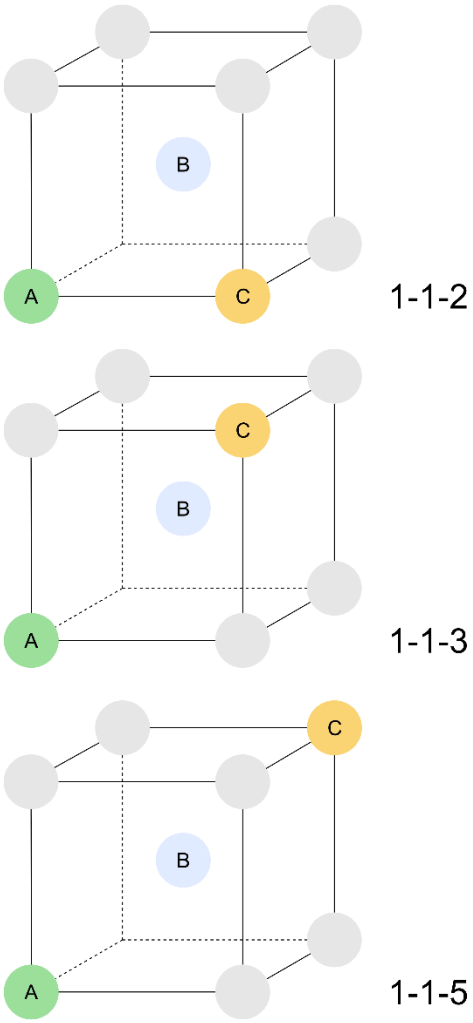

Fig. 3 *– Atomic models of the three triplet structures studied, where Mn, Ni (section 3.2) or a vacancy (section 3.3) is placed in A and B positions and one of Si, Cu, Mn, Ni or a vacancy is substituted in position C on the bcc Fe lattice. Simulations have been run for all permutations.*

Fig. 4 shows the energies of the triplet binding energies calculated using Eq. (1). From comparison with previous literature, it is seen there is poor agreement with this work for clusters containing Mn; this is again attributed to the shallow energy landscape between magnetic moments as discussed in the previous section. For clusters without Mn, our findings are in line with previous works to within the error of DFT (~0.1 eV). For the study by Bonny *et al.* [51] that concentrated on clusters in the 1-1-2 configuration, agreement was found to be within 0.1 eV for all but the Mn-Mn-Mn, Vac-Mn-Mn, Mn-Mn-Ni and Ni-Cu-Mn (ordered A-B-C in Fig. 3), which is again attributed to the shallow energy landscape of Mn. It is evident that clusters consisting only of Mn are energetically unfavourable, as are Mn-Mn-Ni clusters, which are repulsive (up to 0.34 eV) for all configurations studied. With an increase in Ni content of the clusters to 2Ni:1Mn, clusters become more favourable, however, the magnitudes of their interaction are very small (between 0.02 and -0.08 eV). It is also interesting to note that modelling different configurations and orderings is important as only modelling a single 1-1-2 configuration could be misleading. Examples of this are clear in Fig. 4 where Mn-Ni-X clusters show differing behaviour in the 1-1-2 configuration when compared to the 1-1-3 or 1-1-5 configurations and in some cases, such as for Mn-Ni-Ni triplets, the 0.09 eV repulsion becomes a marginal attraction, albeit within the uncertainty of DFT methods. Equally, the 1-1-5 configurations can be more repulsive by a significant margin than the 1-1-2 configurations; examples of this are the Mn-Mn-Mn and Mn-Mn-Ni clusters.

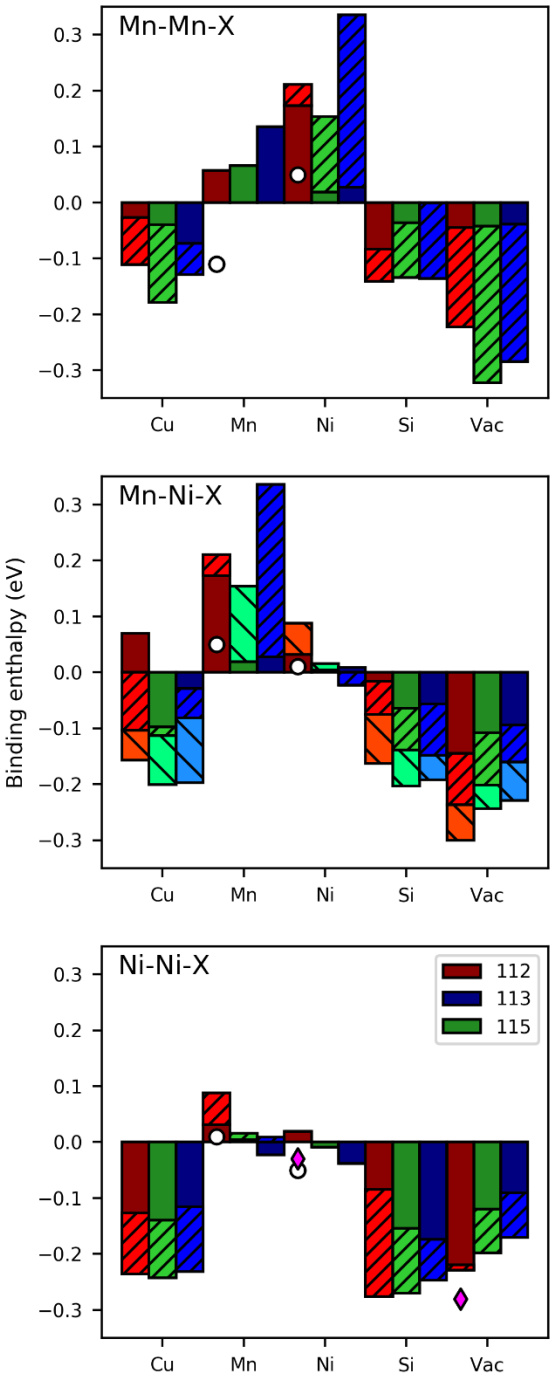

Fig. 4 *– Binding enthalpies of each of the triplet clusters in the different positions shown in Fig. 3. Each line on the bars represent the energies of the specified cluster composition (e.g. Cu-Mn-Ni) and configurations (e.g. 1-1-3) in different permutations. For example, Cu-Mn-Ni (1-1-3) triplets have three distinct configurations whereas Mn-Mn-Mn (1-1-3) triplets only have one distinct configuration. Results from Bonny et al.* [48] *(white circles) and Bonny et al.* [50] *(purple diamonds) are shown for comparison.*

It is clear that Cu, Si and vacancies are important for the stability of small, local Mn- and Ni-containing clusters, as we have found pure substitutional Mn-Ni triplet clusters to be repulsive or only weakly bound in the absence of a SIA; although a previous study by Bonny *et al.* found that quadruplets and larger clusters of Mn and Ni may be more stable [48]. While there are many variables that drive cluster formation that are neglected here such as temperature, strain, defect fluxes and

defect sinks; our results suggest that Cu, Si and vacancies will increase the thermodynamic stability of clusters and could be directly used to parameterise KMC codes that can better take into account these factors. The Cu content in modern Grade 3 A508 RPV steels is low (typically < 0.1 at %), and Cu phase separates early in the lifetime of the reactor ($<10^{23}$ n m^{-2} fluence, ≥1 MeV) [69]. Due to the established flux-coupling effect of vacancy drag of Ni, Mn and Si to existing Cu clusters [3,27,70] and the strong binding energy (-0.2 eV) of Cu-Ni-Mn triplets, existing Cu clusters will act locally as nucleation points for Mn-Ni clusters, evidence for this is seen experimentally with the observation of Cu-rich cores surrounded by Mn-Ni-Si rich shells [5,36–38,71]. The availability of Si (0.2 - 0.6 at. %) is typically greater than Cu in the Fe matrix of RPV steels during cluster evolution [3,72–74] and is well below its solubility limit at 500 K [75], therefore it will be more readily available in the matrix than Cu during the operation of the RPV. Due to the availability of Si, the established solute transport of Mn, Ni and Si by both vacancies and SIAs to sinks (such as interstitial loops and dislocations) [8,39,40,70] and the strong binding energy of Si with Mn/Ni in pairs and triplets, Si will increase the thermodynamic driving force for solute clustering. The stronger binding energies of the Si-containing triplet clusters are likely due to its semi-metallic nature and smaller atomic radius (110 pm compared to 140 pm for Mn and Fe, and 135 pm for Ni and Cu [76]), and its strong binding with vacancies and other solutes in 1nn position [13,49,68]. Electronic interactions of Si with Fe and other solutes may also play a role, as these have been found to be largely responsible for its solubility in *bcc* Fe rather than size effects [10]. Si also exhibits remarkably strong vacancy-solute drag factors [14], and Si-vacancy complexes have been experimentally observed to form and evolve as Si can stabilise vacancy clusters; however, solute aggregation of pure Si clusters close to vacancy clusters is not found to occur in model alloys (i.e. it has been found experimentally that Si clusters must contain vacancies within them to be stable, rather than nucleating on vacancy clusters and forming a separate phase as is seen for Cu [41]).

Solute-vacancy complexes are well-known forms of radiation induced features that have been observed in Fe-Mn and Fe-Ni model alloys [41]. The binding of Mn and Ni to vacancies is significant and both are known to exhibit vacancy-solute drag up to temperatures of ~ 1000 K in *bcc* Fe [13]). Therefore, the results of the current study for favourable binding energies of Mn-Mn-vacancy clusters (max. -0.32 eV), Mn-Ni-vacancy (max. -0.30 eV), and Ni-Ni-vacancy (max. -0.23 eV) are no surprise. These results suggest that on a local scale, greater concentrations of vacancies (as a result of larger fluence) will lead to more cluster nucleation; this is in good agreement with the observed relationship between neutron fluence and cluster growth that higher fluence increases number density of clusters [27,31,77,78].

To better determine the role of each species in cluster stability, the local density of states (LDOS) of Mn and Ni at 1nn separation from different solute species and a vacancy in bulk *bcc* Fe is shown in Fig. 5. It is clear to see that the shape and position of the Mn LDOS are similar when isolated and in the presence of a stabilising species (Cu, Si and vacancy). Here, the anti-bonding peak in the upper spin channel is unfilled (above the Fermi level). This is in contrast to the LDOS of Mn in the presence of a destabilising species (Mn or Ni) which display the higher energy states in the upper spin channel as filled. This suggests that there is a repulsive interaction and similar observations have been made for Mn when in the presence of defects in *bcc* Fe [66,79]. For Ni-X pairs, the LDOS around the Ni is very similar when isolated in *bcc* Fe or in the presence of any of the studied solutes. It is evident that the cause of the variance in stability, by the other solute species, is difficult to observe locally. It is possible that the differing stability can be explained by the effective size of the solute species (related to d-band occupation), which provides some indication of the relative strain imposed on the system. Moreover, vacancies and Si are undersized, and Ni and Mn are oversized, when compared to the Fe lattice [57,80,81]. Therefore, an alleviation of strain will be achieved by the combination of the former with the latter two.

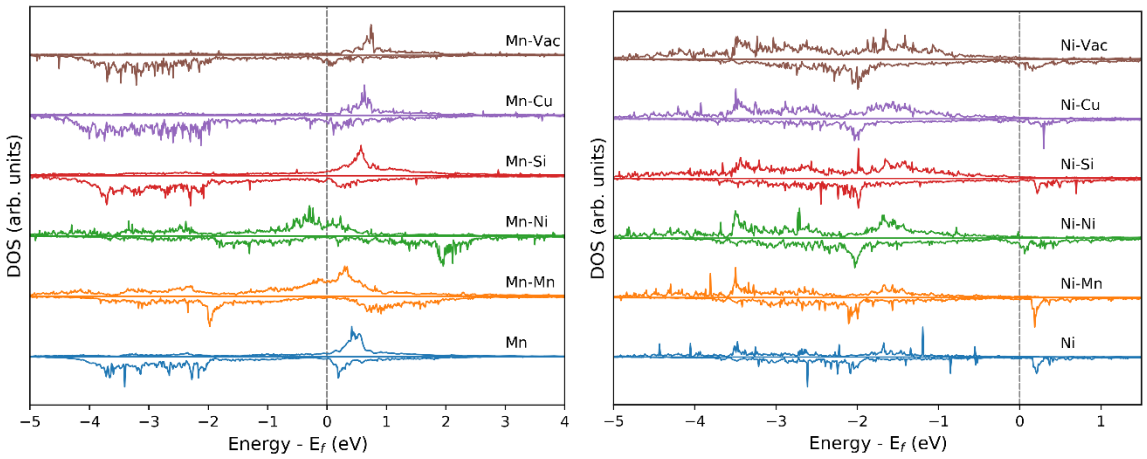

Fig. 5 *– Local density of states of (a) Mn and (b) Ni in* bcc *Fe when in 1nn positions to a vacancy, Cu, Si, Ni or Mn atom. Dashed line denotes Fermi energy.*

In atom probe experiments, solute clusters are frequently found in welds and close to dislocation loops or grain boundaries [39,40,78,82,83]. It should be noted that the analysis in this work does not consider strained environments such as those found near these regions nor the increased solute concentrations found in welds where Ni content can be up to 1.6 at. % [3,73]. However, it is known that dislocations and grain boundaries act as sinks for vacancies and that Cu, Mn, Ni and Si will enrich at ground boundaries due to vacancy drag and SIA migration (particularly for Mn) [13,25,57,58,70]; this, combined with the strong binding energies for triplet clusters including vacancies, will facilitate nucleation and growth of clusters in these regions.

3.3 Divacancy triplet clusters

As solute drag by vacancies has been found to be very strong at RPV temperatures for Mn, Si, Ni and Cu [13], investigations have been made to better understand the binding between the solutes and vacancies by calculating the binding energies of triplets including two vacancies, see Fig. 6. Good agreement is found between our findings and those of previous works, clusters containing two vacancies and only one Ni or Mn are strongly bound and up to -0.25 eV more energetically favourable than Mn or Ni clusters containing only one vacancy, suggesting that if the vacancy concentration is high enough, Ni-Mn-vacancy clusters will readily form. For divacancy clusters containing Si or Cu, the binding energy is very strong, and in excess of -0.5 eV for the compact 1-1-2 configurations, so Si and Cu will strongly bind to vacancies and migrate via this pathway (more so than Ni and Mn), in agreement with previous work that has found solute drag is strong at RPV temperature and drives formation of solute-defect clusters [13,84]. Indeed, Si and Cu divacancy triplets have stronger binding energies than pure vacancy triplets for all configurations studied, suggesting that there is a solute-vacancy synergy that can occur both ways, i.e. solutes can stabilise vacancy clusters as well as vacancies stabilising solute clusters, in agreement with experimental observations that irradiation induced vacancies are stabilized by forming vacancy-solute complexes [41]. However, from studies of triplet clusters alone it is difficult to say whether Si and Cu may act as vacancy traps as previous works have found both that the presence of solutes can stabilise vacancy clusters [13], but also that large solute clusters (of Cu) are more mobile than single atoms [85].

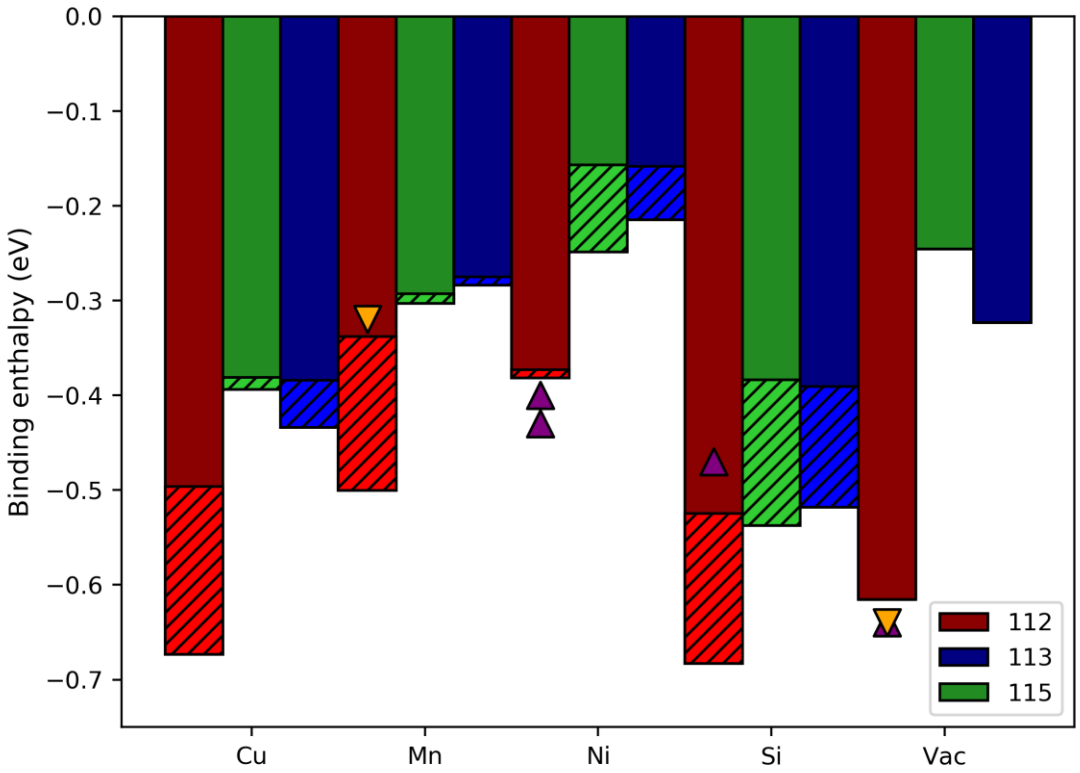

Fig. 6 *– Binding enthalpies of triplet clusters containing two vacancies, in the different configurations shown in Fig. 3. compared with previous works by Bakaev et al.* [49] *(orange inverted triangles) and Bonny et al.* [50] *(purple triangles).*

The findings from sections 3.2 and 3.3 suggest that locally, vacancies, Cu and Si will aid initial cluster growth due to the attractive binding energy of triplets and pairs that include these species. However, in order to extrapolate further, higher order codes such as KMC are required to model larger system sizes and study cluster evolution and so it is suggested that these results are used in parameterisation of future models. Due to the complexity of RPV alloys, there will be many distinct species present and clusters will also have significant Fe content [20,86,87] and so when modelling triplet clusters, the configurational shape, chemistry and ordering of the triplet is also important. Finally, considering there is strong evidence that interstitial loops can act as nucleation points for the growth of solute clusters [39,43,88], it is likely that the energetic drive for clustering is a combination of interstitial loops, Cu precipitates and vacancy clusters.

3.4 Importance of three-body interaction

In order to model the evolution of solutes in the *bcc* Fe system, larger scale models, in particular KMC, have been used to study cluster growth. Due to the computational expense of the DFT calculations used to parameterize KMC codes, DFT-Monte Carlo simulations so far have only taken into account pair-wise interactions, for example Refs. [23–26]. In this section we address this issue by explicitly calculating the binding energies predicted from purely pairwise interactions and comparing them with the triplet binding energies.

Fig. 7 quantifies error associated with the 3-body binding energy when only using the pair-wise interactions given by Eq. (3) to describe triplet clusters. For the clusters containing no vacancies, the least deviations in binding energies are observed ($|\Delta E_b| < \sim 0.1$ eV); of those that deviate, the majority of the binding energies are underestimated by the pair-wise calculations alone. Where one or

two vacancies are present, all but two points in Fig. 7 show underestimates of the binding energies of up to 0.3 eV for both repulsion and attraction. Therefore, by only taking pairwise interactions into account in previous works, there will have been a bias for cluster formation around interstitial loops rather than vacancy clusters in KMC codes and a subsequent underestimation of the impact vacancy clusters can have on the nucleation and growth of solute clusters could have been made. Indeed, solute drag by vacancies is important for migration of all solutes under consideration [13] as well as the role of SIAs. It is therefore reasonable to deduce that the three-body terms should be used for parameterisation of future models in parallel with the recent results from SIA models for a more accurate model of cluster behaviour.

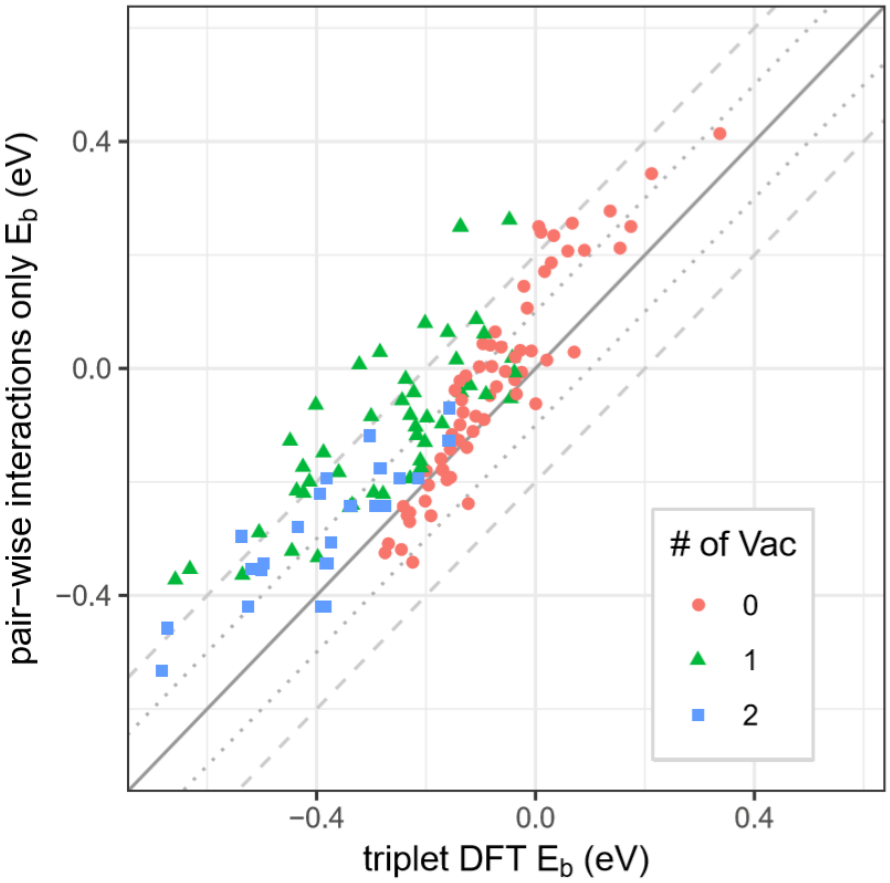

Fig. 7 *Magnitude of three-body interaction in triplet clusters; defined as the difference in binding energies between explicit DFT calculation of triplets (x-axis) and combination of pair-wise binding energies (also from DFT, y-axis). Colour coded by number of vacancies in the cluster. Dotted and dashed lines represent deviation of ±0.1 eV and ±0.2 eV respectively.*

4. Conclusions

To summarise, our main findings are:

1. Triplet clusters containing exclusively Mn and/or Ni are not energetically stable and so cluster growth will involve vacancies, Cu, Si or SIAs.
2. All solutes bind strongly to vacancies and may act as vacancy traps, additionally, a synergetic effect is seen whereby solutes stabilise vacancy clusters (as well as vacancies stabilising solute clusters).

3. Binding energies of triplet clusters predicted from purely pair binding energies are nearly all underestimated by not including a 3-body term and the underestimation is worse for triplets containing vacancies where differences of 0.3 eV were found. This will have led to a bias of formation of clusters on interstitial loops rather than vacancy clusters.
4. The energetics of the 3-body term (or explicitly calculated triplet energies) should be included in future KMC models to improve the accuracy of predictions as important energetics are neglected by only taking solute pairs into account.

Supplementary Material

See supplementary material for DFT binding energies of all triplets and pairs.

Acknowledgements

TMW acknowledges financial support from Rolls-Royce Plc and through the EPSRC Centre for Doctoral training in Nuclear Energy (EP/L015900/1), Daniel King and Mark Wenman acknowledge funding from EPSRC (EP/P005101/1). This research was undertaken with the assistance of resources provided by the EPSRC Tier 2 allocation on CSD3 (Skylake and KNL) HPCs, Australian National Computational Infrastructure provided by UNSW (Raijin) and Imperial College Tier 2 computing (Cx1 and Cx2)

References

[1] J.M. Hyde, D. Ellis, C.A. English, T.J. Williams, Effects of Radiation on Materials : 20th International Symposium, 2001.

[2] J.F. Knott, C.A. English, Views of TAGSI on the principles underlying the assessment of the mechanical properties of irradiated ferritic steel Reactor Pressure Vessels, Int. J. Press. Vessel. Pip. 76 (1999) 891–908. doi:10.1016/S0308-0161(99)00068-X.

[3] M.K. Miller, K.A. Powers, R.K. Nanstad, P. Efsing, Atom probe tomography characterizations of high nickel , low copper surveillance RPV welds irradiated to high fluences, J. Nucl. Mater. 437 (2013) 107–115. doi:10.1016/j.jnucmat.2013.01.312.

[4] M. Miller, K. Russell, Embrittlement of RPV steels : An atom probe tomography perspective, J. Nucl. Mater. 371 (2007) 145–160. doi:10.1016/j.jnucmat.2007.05.003.

[5] J.M. Hyde, G. Sha, E.A. Marquis, A. Morley, K.B. Wilford, T.J. Williams, A comparison of the structure of solute clusters formed during thermal ageing and irradiation, Ultramicroscopy. 111 (2011) 664–671. doi:10.1016/j.ultramic.2010.12.030.

[6] P. Auger, P. Pareige, M. Akamatsu, J.-C. Van Duysen, Microstructural characterization of atom clusters in irradiated pressure vessel steels and model alloys, J. Nucl. Mater. 211 (1994) 194–201. doi:10.1016/0022-3115(94)90347-6.

[7] C. Brillaud, F. Hedin, In-service evaluation of french pressurized water reactor vessel steel, Eff. Radiat. Mater. 15th Int. Symp. (1992) 23–49.

[8] M.K. Miller, M.A. Sokolov, R.K. Nanstad, K.F. Russell, APT characterization of high nickel RPV steels, J. Nucl. Mater. 351 (2006) 187–196. doi:10.1016/j.jnucmat.2006.02.013.

[9] G. Bonny, R.C. Pasianot, L. Malerba, Fe–Ni many-body potential for metallurgical applications, Model. Simul. Mater. Sci. Eng. 17 (2009). doi:10.1088/0965-0393/17/2/025010.

[10] T. Ohnuma, N. Soneda, M. Iwasawa, First-principles calculations of vacancy – solute element interactions in body-centered cubic iron, Acta Mater. 57 (2009) 5947–5955. doi:10.1016/j.actamat.2009.08.020.

[11] O. Gorbatov, P. Korzhavyi, A. Ruban, B. Johansson, Y. Gornostyrev, Vacancy–solute

interactions in ferromagnetic and paramagnetic bcc iron: Ab initio calculations, J. Nucl. Mater. 419 (2011) 248–255. doi:10.1016/j.jnucmat.2011.09.002.

[12] P.D. Styman, J.M. Hyde, K. Wilford, G.D.W. Smith, Quantitative methods for the APT analysis of thermally aged RPV steels, Ultramicroscopy. 132 (2013) 258–264. doi:10.1016/j.ultramic.2012.12.003.

[13] L. Messina, M. Nastar, T. Garnier, C. Domain, P. Olsson, Exact ab initio transport coefficients in bcc Fe-X (X=Cr, Cu, Mn, Ni, P, Si) dilute alloys, Phys. Rev. B. 90 (2014) 104203. doi:10.1103/PhysRevB.90.104203.

[14] C. Domain, C.S. Becquart, Solute - $<111>$ interstitial loop interaction in α-Fe: A DFT study, J. Nucl. Mater. 499 (2018) 582–594. doi:10.1016/j.jnucmat.2017.10.070.

[15] D.J.M. King, P.A. Burr, S.C. Middleburgh, T.M. Whiting, M.G. Burke, M.R. Wenman, The formation and structure of Fe-Mn-Ni-Si solute clusters and G-phase precipitates in steels, J. Nucl. Mater. 505 (2018) 1–6. doi:10.1016/j.jnucmat.2018.03.050.

[16] B.D. Wirth, G.R. Odette, W.A. Pavinch, G.E. Lucas, S.E. Spooner, Small Angle Neutron Scattering Study of Linde 80 RPV Welds, in: Eff. Radiat. Mater. 18th Int. Symp. ASTM STP 1325, 1999: p. 102. doi:10.1017/CBO9781107415324.004.

[17] G. Odette, On the dominant mechanism of irradiation embrittlement of reactor pressure vessel steels, Scr. Metall. 17 (1983) 1183–1188. doi:10.1016/0036-9748(83)90280-6.

[18] R. Chaouadi, R. Gérard, Copper precipitate hardening of irradiated RPV materials and implications on the superposition law and re-irradiation kinetics, J. Nucl. Mater. 345 (2005) 65–74. doi:10.1016/j.jnucmat.2005.05.001.

[19] W.J. Phythian, C.A. English, Microstructural evolution in reactor pressure vessel steels, J. Nucl. Mater. 205 (1993) 162–177. doi:10.1016/0022-3115(93)90079-E.

[20] C.L. Liu, G.R. Odette, B.D. Wirth, G.E. Lucas, A lattice Monte Carlo simulation of nanophase compositions and structures in irradiated pressure vessel Fe-Cu-Ni-Mn-Si steels, Mater. Sci. Eng. A. 238 (1997) 202–209. doi:10.1016/S0921-5093(97)00450-4.

[21] G.R. Odette, G.E. Lucas, Recent progress in understanding reactor pressure vessel steel embrittlement, Radiat. Eff. Defects Solids. 144 (1998) 189–231. doi:10.1080/10420159808229676.

[22] G. Odette, B. Wirth, A computational microscopy study of nanostructural evolution in irradiated pressure vessel steels, J. Nucl. Mater. 251 (1997) 157–171. doi:10.1016/S0022-3115(97)00267-5.

[23] E. Vincent, C.S. Becquart, C. Domain, Atomic kinetic Monte Carlo model based on ab initio data: Simulation of microstructural evolution under irradiation of dilute Fe-CuNiMnSi alloys, Nucl. Instruments Methods Phys. Res. Sect. B Beam Interact. with Mater. Atoms. 255 (2007) 78–84. doi:10.1016/j.nimb.2006.11.033.

[24] E. Vincent, C.S. Becquart, C. Domain, Microstructural evolution under high flux irradiation of dilute Fe-CuNiMnSi alloys studied by an atomic kinetic Monte Carlo model accounting for both vacancies and self interstitials, J. Nucl. Mater. 382 (2008) 154–159. doi:10.1016/j.jnucmat.2008.08.019.

[25] R. Ngayam-Happy, C.S. Becquart, C. Domain, L. Malerba, Formation and evolution of MnNi clusters in neutron irradiated dilute Fe alloys modelled by a first principle-based AKMC method, J. Nucl. Mater. 426 (2012) 198–207. doi:10.1016/j.jnucmat.2012.03.033.

[26] R. Ngayam-happy, C.S. Becquart, C. Domain, First principle-based AKMC modelling of the formation and medium-term evolution of point defect and solute-rich clusters in a neutron

irradiated complex Fe – CuMnNiSiP alloy representative of reactor pressure vessel steels, J. Nucl. Mater. 440 (2013) 143–152. doi:10.1016/j.jnucmat.2013.04.081.

[27] P. Wells, T. Yamamoto, B. Miller, T. Milot, J. Cole, Y. Wu, G.R. Odette, Evolution of manganese–nickel–silicon-dominated phases in highly irradiated reactor pressure vessel steels, Acta Mater. 80 (2014) 205–219. doi:10.1016/j.actamat.2014.07.040.

[28] E. Meslin, B. Radiguet, P. Pareige, A. Barbu, Kinetic of solute clustering in neutron irradiated ferritic model alloys and a French pressure vessel steel investigated by atom probe tomography, J. Nucl. Mater. 399 (2010) 137–145. doi:10.1016/j.jnucmat.2009.11.012.

[29] S. V Fedotova, E.A. Kuleshova, B.A. Gurovich, A.S. Frolov, D.A. Maltsev, G.M. Zhuchkov, I. V Fedotov, APT-studies of phase formation features in VVER-440 RPV weld and base metal in irradiation-annealing cycles, J. Nucl. Mater. 511 (2018) 30–42. doi:10.1016/j.jnucmat.2018.08.046.

[30] K. Lindgren, M. Boåsen, K. Stiller, P. Efsing, M. Thuvander, Cluster formation in in-service thermally aged pressurizer welds, J. Nucl. Mater. 504 (2018) 23–28. doi:10.1016/j.jnucmat.2018.03.017.

[31] K. Lindgren, M. Boåsen, K. Stiller, P. Efsing, M. Thuvander, Evolution of precipitation in reactor pressure vessel steel welds under neutron irradiation, J. Nucl. Mater. 488 (2017) 222–230. doi:10.1016/j.jnucmat.2017.03.019.

[32] K. Lindgren, K. Stiller, P. Efsing, M. Thuvander, On the Analysis of Clustering in an Irradiated Low Alloy Reactor Pressure Vessel Steel Weld, (2019) 376–384. doi:10.1017/S1431927617000162.

[33] P.D. Styman, J.M. Hyde, D. Parfitt, K. Wilford, M.G. Burke, C.A. English, P. Efsing, Post-irradiation annealing of Ni-Mn-Si-enriched clusters in a neutron-irradiated RPV steel weld using Atom Probe Tomography, J. Nucl. Mater. 459 (2015) 127–134. doi:10.1016/j.jnucmat.2015.01.027.

[34] J.E. Zelenty, Understanding thermally induced embrittlement in low copper RPV steels utilising atom probe tomography, Mater. Sci. Technol. 31 (2015) 981–988. doi:10.1179/1743284714Y.0000000718.

[35] P.D. Styman, Atomic scale studies of thermally aged reactor pressure vessel steels, Oxford University, 2012.

[36] M.K. Miller, B.D. Wirth, G.R. Odette, Precipitation in neutron-irradiated Fe–Cu and Fe–Cu–Mn model alloys: a comparison of APT and SANS data, Mater. Sci. Eng. A. 353 (2003) 133–139. doi:10.1016/S0921-5093(02)00679-2.

[37] G.R. Odette, C.L. Liu, B.D. Wirth, On the Composition and Structure of Nanoprecipitates in Irradiated Pressure Vessel Steels, in: MRS Symp. Proc. 439, 1997: p. 457.

[38] E.D. Eason, G.R. Odette, R.K. Nanstad, T. Yamamoto, A physically based correlation of irradiation-induced transition temperature shifts for RPV steels, Oak Ridge Natl. Lab. (2006). http://info.ornl.gov/sites/publications/files/Pub2592.pdf.

[39] E. Meslin, B. Radiguet, M. Loyer-Prost, Radiation-induced precipitation in a ferritic model alloy: An experimental and theoretical study, Acta Mater. 61 (2013) 6246–6254. doi:10.1016/j.actamat.2013.07.008.

[40] E. Meslin, M. Lambrecht, M. Hernández-Mayoral, F. Bergner, L. Malerba, P. Pareige, B. Radiguet, A. Barbu, D. Gómez-Briceño, A. Ulbricht, A. Almazouzi, Characterization of neutron-irradiated ferritic model alloys and a RPV steel from combined APT, SANS, TEM and PAS analyses, J. Nucl. Mater. 406 (2010) 73–83. doi:10.1016/j.jnucmat.2009.12.021.

[41] Y. Nagai, K. Takadate, Z. Tang, H. Ohkubo, H. Sunaga, H. Takizawa, M. Hasegawa, Positron annihilation study of vacancy-solute complex evolution in Fe-based alloys, Phys. Rev. B. 67 (2003) 2–7. doi:10.1103/PhysRevB.67.224202.

[42] S. Glade, B. Wirth, G. Odette, P. Asoka-Kumar, Positron annihilation spectroscopy and small angle neutron scattering characterization of nanostructural features in high-nickel model reactor pressure vessel steels, J. Nucl. Mater. 351 (2006) 197–208. doi:10.1016/j.jnucmat.2006.02.012.

[43] L.T. Belkacemi, E. Meslin, B. Décamps, B. Radiguet, J. Henry, Radiation-induced bcc-fcc phase transformation in a Fe–3%Ni alloy, Acta Mater. 161 (2018) 61–72. doi:10.1016/j.actamat.2018.08.031.

[44] M. Hernandez-Mayoral, D. Gomez-Briceno, Transmission electron microscopy study on neutron irradiated pure iron and RPV model alloys, J. Nucl. Mater. 399 (2010) 146–153. doi:10.1016/j.jnucmat.2009.11.013.

[45] M. Chiapetto, L. Messina, C.S. Becquart, P. Olsson, L. Malerba, Nanostructure evolution of neutron-irradiated reactor pressure vessel steels : Revised Object kinetic Monte Carlo model, Nucl. Inst. Methods Phys. Res. B. 393 (2017) 105–109. doi:10.1016/j.nimb.2016.09.025.

[46] P. Olsson, C.S. Becquart, C. Domain, Ab initio threshold displacement energies in iron, Mater. Res. Lett. 0 (2016) 1–7. doi:10.1080/21663831.2016.1181680.

[47] G. Bonny, R.C. Pasianot, N. Castin, L. Malerba, Ternary Fe–Cu–Ni many-body potential to model reactor pressure vessel steels: First validation by simulated thermal annealing, Philos. Mag. 89 (2009) 3531–3546. doi:10.1080/14786430903299824.

[48] G. Bonny, D. Terentyev, a. Bakaev, E.E. Zhurkin, M. Hou, D. Van Neck, L. Malerba, On the thermal stability of late blooming phases in reactor pressure vessel steels: An atomistic study, J. Nucl. Mater. 442 (2013) 282–291. doi:10.1016/j.jnucmat.2013.08.018.

[49] A. Bakaev, D. Terentyev, G. Bonny, T.P.C. Klaver, P. Olsson, D. Van Neck, Interaction of minor alloying elements of high-Cr ferritic steels with lattice defects: An ab initio study, J. Nucl. Mater. 444 (2014) 237–246. doi:10.1016/j.jnucmat.2013.09.053.

[50] G. Bonny, A. Bakaev, P. Olsson, C. Domain, E.E. Zhurkin, M. Posselt, Interatomic potential to study the formation of NiCr clusters in high Cr ferritic steels, J. Nucl. Mater. 484 (2017) 42–50. doi:10.1016/j.jnucmat.2016.11.017.

[51] G. Bonny, C. Domain, N. Castin, P. Olsson, L. Malerba, The impact of alloying elements on the precipitation stability and kinetics in iron based alloys: An atomistic study, Comput. Mater. Sci. 161 (2019) 309–320. doi:10.1016/j.commatsci.2019.02.007.

[52] S. Shu, P.B. Wells, N. Almirall, G.R. Odette, D.D. Morgan, Thermodynamics and kinetics of core-shell versus appendage co- precipitation morphologies : An example in the Fe-Cu-Mn-Ni-Si system, Acta Mater. 157 (2018) 298–306. doi:10.1016/j.actamat.2018.07.037.

[53] S. Shu, P.B. Wells, N. Almirall, G.R. Odette, D.D. Morgan, Thermodynamics and kinetics of core-shell versus appendage co- precipitation morphologies : An example in the Fe-Cu-Mn-Ni-Si system, Acta Mater. 157 (2018) 298–306. doi:10.1016/j.actamat.2018.07.037.

[54] R. Ngayam-happy, P. Olsson, C.S. Becquart, C. Domain, Isochronal annealing of electron-irradiated dilute Fe alloys modelled by an ab initio based AKMC method : Influence of solute – interstitial cluster properties, J. Nucl. Mater. 407 (2010) 16–28. doi:10.1016/j.jnucmat.2010.07.004.

[55] S. Hocker, P. Binkele, S. Schmauder, Precipitation in α -Fe based Fe-Cu-Ni-Mn-alloys : behaviour of Ni and Mn modelled by ab initio and kinetic Monte Carlo simulations, (2014) 679–687. doi:10.1007/s00339-013-7850-9.

[56] A. Cerezo, S. Hirosawa, I. Rozdilsky, G.D.W. Smith, Combined atomic-scale modelling and experimental studies of nucleation in the solid state, Philos. Trans. R. Soc. A. 361 (2003) 463–477.

[57] P. Olsson, T. Klaver, C. Domain, Ab initio study of solute transition-metal interactions with point defects in bcc Fe, Phys. Rev. B. 81 (2010) 054102. doi:10.1103/PhysRevB.81.054102.

[58] E. Vincent, C.S. Becquart, C. Domain, Ab initio calculations of self-interstitial interaction and migration with solute atoms in bcc Fe, J. Nucl. Mater. 359 (2006) 227–237. doi:10.1016/j.jnucmat.2006.08.022.

[59] G. Kresse, J. Hafner, Ab initio molecular-dynamics simulation of the liquid-metal–amorphous-semiconductor transition in germanium, Phys. Rev. B. 49 (1994) 14251–14269. doi:10.1103/PhysRevB.49.14251.

[60] G. Kresse, From ultrasoft pseudopotentials to the projector augmented-wave method, Phys. Rev. B. 59 (1999) 1758–1775. doi:10.1103/PhysRevB.59.1758.

[61] G. Kresse, J. Hafner, Ab initio molecular dynamics for liquid metals, Phys. Rev. B. 47 (1993) 558–561. doi:10.1103/PhysRevB.47.558.

[62] G. Kresse, J. Furthmüller, Efficiency of ab-initio total energy calculations for metals and semiconductors using a plane-wave basis set, Comput. Mater. Sci. 6 (1996) 15–50. doi:10.1016/0927-0256(96)00008-0.

[63] P.E. Blöchl, Projector augmented-wave method, Phys. Rev. B. 50 (1994) 17953–17979. doi:10.1103/PhysRevB.50.17953.

[64] J.P. Perdew, K. Burke, M. Ernzerhof, Generalized Gradient Approximation Made Simple, Phys. Rev. Lett. 77 (1996) 3865–3868. doi:10.1103/PhysRevLett.77.3865.

[65] M. Methfessel, A.T. Paxton, High-precision sampling for Brillouin-zone integration in metals, Phys. Rev. B. 40 (1989) 3616–3621. doi:10.1103/PhysRevB.40.3616.

[66] D.J.M. King, S.C. Middleburgh, P.A. Burr, T.M. Whiting, P.C. Fossati, M.R. Wenman, Density functional theory study of the magnetic moment of solute Mn in bcc Fe, Phys. Rev. B. 98 (2018) 024418. doi:10.1103/PhysRevB.98.024418.

[67] E. Vincent, C. Becquart, C. Domain, Ab initio calculations of vacancy interactions with solute atoms in bcc Fe, Nucl. Instruments Methods Phys. Res. Sect. B. 228 (2005) 137–141. doi:10.1016/j.nimb.2004.10.035.

[68] A. Bakaev, D. Terentyev, X. He, D. Van Neck, Synergetic effects of Mn and Si in the interaction with point defects in bcc Fe, J. Nucl. Mater. 455 (2014) 5–9. doi:10.1016/j.jnucmat.2014.02.033.

[69] B.D. Wirth, G.R. Odette, W.A. Pavinich, G.E. Lucas, S.E. Spooner, Effects of Radiation on Materials: 18th International Symposium, 1999. doi:10.1520/STP1325-EB.

[70] L. Messina, M. Nastar, N. Sandberg, P. Olsson, Systematic electronic-structure investigation of substitutional impurity diffusion and flux coupling in bcc iron, Phys. Rev. B. 93 (2016) 1–18. doi:10.1103/PhysRevB.93.184302.

[71] P.D. Styman, J.M. Hyde, K. Wilford, D. Parfitt, N. Riddle, G.D.W. Smith, Characterisation of interfacial segregation to Cu-enriched precipitates in two thermally aged reactor pressure vessel steel welds, Ultramicroscopy. 159 (2015) 292–298. doi:10.1016/j.ultramic.2015.05.013.

[72] M.K. Miller, M.G. Burke, An atom probe field ion microscopy study of neutron-irradiated pressure vessel steels, J. Nucl. Mater. 195 (1992) 68–82. doi:10.1016/0022-3115(92)90364-Q.

[73] M.K. Miller, a. a. Chernobaeva, Y.I. Shtrombakh, K.F. Russell, R.K. Nanstad, D.Y. Erak,

O.O. Zabusov, Evolution of the nanostructure of VVER-1000 RPV materials under neutron irradiation and post irradiation annealing, J. Nucl. Mater. 385 (2009) 615–622. doi:10.1016/j.jnucmat.2009.01.299.

[74] P. Pareige, J.C. Van Duysen, P. Auger, An APFIM study of the microstructure of a ferrite alloy after high fluence neutron irradiation, Appl. Surf. Sci. 67 (1993) 342–347. doi:10.1016/0169-4332(93)90336-A.

[75] L. Kaufman, Coupled phase diagrams and thermochemical data for transition metal binary systems-VI, Calphad. 3 (1979) 45–76.

[76] J.C. Slater, Atomic radii in crystals, J. Chem. Phys. 41 (1964) 3199–3204. doi:10.1063/1.1725697.

[77] F. Bergner, a. Ulbricht, H.-W. Viehrig, Acceleration of irradiation hardening of low-copper reactor pressure vessel steel observed by means of SANS and tensile testing, Philos. Mag. Lett. 89 (2009) 795–805. doi:10.1080/09500830903304117.

[78] E. Meslin, B. Radiguet, P. Pareige, C. Toffolon, A. Barbu, Irradiation-Induced Solute Clustering in a Low Nickel FeMnNi Ferritic Alloy, Exp. Mech. 51 (2011) 1453–1458. doi:10.1007/s11340-011-9476-1.

[79] V.I. Anisimov, V.P. Antropov, A.I. Liechtenstein, V.A. Gubanov, A. V. Postnikov, Electronic structure and magnetic properties of 3d impurities in ferromagnetic metals, Phys. Rev. B. 37 (1988) 5598–5602. doi:10.1201/b19496-8.

[80] H. King, Quantitative size-factors for metallic solid solutions, J. Mater. Sci. 1 (1966) 79–90. doi:10.1007/BF00549722.

[81] K.A. Gschneidner, Physical Properties and Interrelationships of Metallic and Semimetallic Elements, Solid State Phys. 16 (1964) 275.

[82] S.M. Bruemmer, E.P. Simonen, P.M. Scott, P.L. Andresen, G.S. Was, J.L. Nelson, Radiation-induced material changes and susceptibility to intergranular failure of light-water-reactor core internals, J. Nucl. Mater. 274 (1999) 299–314. doi:10.1016/S0022-3115(99)00075-6.

[83] J.P. Wharry, G.S. Was, A systematic study of radiation-induced segregation in ferritic-martensitic alloys, J. Nucl. Mater. 442 (2013) 7–16. doi:10.1016/j.jnucmat.2013.07.071.

[84] L. Messina, L. Malerba, P. Olsson, Stability and mobility of small vacancy-solute complexes in Fe-MnNi and dilute Fe-X alloys: A kinetic Monte Carlo study, Nucl. Instruments Methods Phys. Res. Sect. B Beam Interact. with Mater. Atoms. 352 (2015) 61–66. doi:10.1016/j.nimb.2014.12.032.

[85] F. Soisson, C.-C. Fu, Cu-precipitation kinetics in alpha-Fe from atomistic simulations: Vacancy-trapping effects and Cu-cluster mobility, Phys. Rev. B. 76 (2007) 214102. doi:10.1103/PhysRevB.76.214102.

[86] A. Morley, G. Sha, S. Hirosawa, A. Cerezo, G.D.W. Smith, Ultramicroscopy Determining the composition of small features in atom probe : bcc Cu-rich precipitates in an Fe-rich matrix, 109 (2009) 535–540. doi:10.1016/j.ultramic.2008.09.010.

[87] F. Soisson, A. Barbu, G. Martin, Monte carlo simulations of copper precipitation in dilute iron-copper alloys during thermal ageing and under electron irradiation, Acta Mater. 44 (1996) 3789–3800.

[88] G. Bonny, D. Terentyev, E.E. Zhurkin, L. Malerba, Monte Carlo study of decorated dislocation loops in FeNiMnCu model alloys, J. Nucl. Mater. 452 (2014) 486–492. doi:10.1016/j.jnucmat.2014.05.051.